frontiers | Frontiers in Oncology

TYPE Original Research
PUBLISHED 02 September 2025
DOI 10.3389/fonc.2025.1627403

OPEN ACCESS

EDITED BY
Yi Ji,
Sichuan University, China

REVIEWED BY
Alfred Otoe Ankrah,
Korle Bu Teaching Hospital, Ghana
Raquel Sánchez Vañó,
La Fe Health Research Institute, Spain

*CORRESPONDENCE
Liang Cai
306663@hospital.cqmu.edu.cn
Shan Wang
wangshan778@163.com

†These authors have contributed equally to this work and share first authorship

RECEIVED 12 May 2025
ACCEPTED 13 August 2025
PUBLISHED 02 September 2025

CITATION
Zhang W, Yang C, Zhao Z, Zhou S, Han Y, Zheng C, Xiong Y, Li C, Zhang Y, Wang Z, Cai L and Wang S (2025) [18F]mFBG PET/CT surpasses [18F]FDG PET/CT for evaluation of pediatric neuroblastoma. *Front. Oncol.* 15:1627403. doi: 10.3389/fonc.2025.1627403

[18F]mFBG PET/CT surpasses [18F]FDG PET/CT for evaluation of pediatric neuroblastoma

Wenqian Zhang[1†], Chao Yang[2†], Zhenzhen Zhao[2], Shunhao Zhou[1], Yanyao Han[1], Chenxi Zheng[1], Yalan Xiong[1], Changchun Li[2], Yao Zhang[2], Zhenni Wang[2], Liang Cai[1*] and Shan Wang[2*]

[1]Department of Nuclear Medicine, The Second Affiliated Hospital of Chongqing Medical University, Chongqing, China, [2]Department of Surgical Oncology, National Clinical Research Center for Child Health and Disorders, Ministry of Education Key Laboratory of Child Development and Disorders, China International Science and Technology Cooperation Base of Child Development and Critical Disorders, Children's Hospital of Chongqing Medical University, Chongqing, China

Purpose: [18F]FDG PET/CT serves as an alternative imaging modality for neuroblastoma in cases where [123I]MIBG yields negative results or is unavailable. [18F]mFBG, a novel PET tracer for neuroblastoma imaging, requires further clinical validation. This preliminary study aims to evaluate the efficacy of [18F]mFBG PET/CT compared to [18F]FDG PET/CT in detecting neuroblastoma.
Methods: In this retrospective investigation, 56 pediatric patients were enrolled. Each patient underwent both [18F]mFBG PET/CT and [18F]FDG PET/CT within one week. Two children underwent a second paired [18F]FDG-[18F]mFBG PET/CT scan. In total, 58 paired scans (mean age 47.6 ± 38.0 months, range 6–108 months) were performed. Two experienced readers measured normal organ uptake (SUV_{mean}), lesion uptake (SUV_{max}), and tumor-to-background ratio (TBR). A lesion-by-lesion analysis was conducted to compare detection rates between [18F]mFBG and [18F]FDG.
Results: Twenty paired scans exhibited negative findings on both [18F]mFBG and [18F]FDG studies. Among the remaining 38 scans, 8 (21.05%) were [18F]mFBG-positive/[18F]FDG-negative, 1 (2.63%) was [18F]FDG-positive/[18F]mFBG-negative, and 29 (76.32%) were positive on both tracers. In these 38 scans, [18F]mFBG PET/CT identified 431 lesions, whereas [18F]FDG PET/CT detected only 162 lesions ($p<0.001$). Six of eight [18F]mFBG-positive/[18F]FDG-negative cases were histopathologically confirmed as neuroblastoma. The mean TBR of [18F]mFBG PET/CT(6.68 ± 5.76) was significantly higher ($p<0.001$) than that of [18F]FDG PET/CT (4.49 ± 2.88).
Conclusion: [18F]mFBG PET/CT detected more neuroblastoma lesions than [18F]FDG PET/CT, suggesting it may be a more viable alternative when standard [123I]MIBG scanning is not feasible.

KEYWORDS

[18F]mFBG, [18F]FDG, norepinephrine transporter, neuroblastoma, PET/CT

Introduction

Neuroblastoma is a malignant solid tumor arising from neural crest, accounting for approximately 8% of pediatric cancers and nearly 15% of cancer-related fatalities in children. Approximately 50% of patients present with soft and/or distant skeletal metastases at diagnosis, a key prognostic factor for poor outcome (1, 2). The 5-year event-free survival rate is typically less than 50% (3, 4), underscoring the critical importance of precise staging for optimal treatment planning and clinical monitoring.

The norepinephrine transporter (NET), a transmembrane protein responsible for norepinephrine reuptake, is highly expressed in neuroblastoma cells. Iodine-123-labeled *meta*-iodobenzylguanidine ([^{123}I]MIBG), a synthetic norepinephrine analogue, is the most widely used radiopharmaceutical for NET imaging (5). Currently, [^{123}I]MIBG planar whole-body scintigraphy remains the gold standard for neuroblastoma nuclear imaging (6–8). However, [^{123}I]MIBG scintigraphy has several limitations, including a 2-day imaging protocol, the need for thyroid blockade, limited spatial resolution, and frequent requirement for procedural sedation during scanning (8, 9). Moreover, only four hospitals in China currently have access to [^{123}I]MIBG.

Positron emission tomography (PET) offers significant advantages over conventional scintigraphy, including shorter scan time, superior sensitivity, higher spatial resolution, and more straightforward radiotracer uptake quantification (10). Several PET tracers have shown promise for neuroblastoma imaging, such as [^{18}F]FDG, [^{18}F]F-DOPA, [^{124}I]MIBG, [^{68}Ga]DOTATATE, with studies demonstrating their ability to detect more tumor lesions compared to paired [^{123}I]MIBG scans (11–14). The NCCN guidelines recommend [^{18}F]FDG PET/CT as second-line imaging for MIBG-negative neuroblastoma cases (7). In China, where [^{123}I]MIBG remains largely unavailable, [^{18}F]FDG PET/CT has become the de facto standard for evaluating neuroblastic tumors and metastatic sites. Studies have demonstrated the clinical utility of [^{18}F]FDG PET/CT in neuroblastoma, reporting higher detection accuracy than [^{123}I]MIBG scintigraphy in selected patient cohorts (15–17). Furthermore, multiple studies have investigated the prognostic relevance of [^{18}F]FDG PET/CT in pediatric neuroblastoma cases (18–20). However, [^{18}F]FDG has limited specificity for skeletal metastases due to high physiological bone marrow uptake, particularly following treatment (8).

Meta-[^{18}F]fluorobenzylguanidine ([^{18}F]mFBG), an MIBG analog, similarly targets NET-expressing cells (21). This tracer has demonstrated favorable safety profiles, biodistribution characteristics, kinetic properties, and lesion detection capability (22). Comparative studies have shown similar physiological and pathological distributions between [^{18}F]mFBG PET/CT and [^{123}I]MIBG scintigraphy, with the former offering superior spatial resolution, improved tumor delineation, and enhanced lesion detection (23–25). Nevertheless, in regions where [^{123}I]MIBG is unavailable, it remains unclear whether [^{18}F]mFBG PET/CT should be prioritized over [^{18}F]FDG PET/CT as the preferred imaging modality.

This preliminary study aims to evaluate the diagnostic performance of [^{18}F]mFBG PET/CT versus [^{18}F]FDG PET/CT in neuroblastoma assessment, seeking to determine its potential as a superior imaging alternative.

Materials and methods

Study design and patients

This retrospective study was conducted following approval by the Institutional Review Board of XXX Hospital from December 2023 to August 2024. Pediatric neuroblastoma patients meeting the following inclusion criteria were enrolled: (a) histopathological confirmed neuroblastoma diagnosis; (b) age > 6 months; (c) legal guardian consent for study participation; (d) ability to complete both [^{18}F]mFBG PET/CT and [^{18}F]FDG PET/CT scans within a 7-day interval; and (e) no therapeutic interventions between scans. Exclusion criteria included pregnancy. Written informed consent was obtained from all legal guardians and from patients aged >8 years. The histopathological analysis was utilized as the primary diagnostic reference standard. For lesions inaccessible to biopsy, clinical follow-up data supplemented by conventional imaging (CT/MRI) as secondary reference standards were utilized.

[^{18}F]mFBG PET/CT and [^{18}F]FDG PET/CT imaging

The synthesis method for [^{18}F]mFBG has been previously documented (26). The imaging studies were performed utilizing a time-of-flight (TOF) and point spread function (PSF) PET/CT scanner (uMI780, Shanghai United Imaging Healthcare Co., LTD, China). Both radiotracers ([^{18}F]mFBG and [^{18}F]FDG) were administered via slow intravenous injection at a dose of 2 MBq/kg (minimum activity: 20 MBq), followed by saline flush,with no fasting requirement for [^{18}F]mFBG imaging. PET acquisition commenced ≥60 minutes post-injection with a 2-minute acquisition per bed position (25), preceded by a low-dose CT scan (80–100 kV, 30–50 mAs) for attenuation correction (24, 25). Images reconstruction employed an ordered subsets expectation maximization algorithm (2 iterations, 10 subsets) with corrections for CT-based attenuation, decay, random events, and scatter, yielding final PET images with 1.5 mm slice thickness.

Lesion detection and image interpretation

Two experienced nuclear medicine physicians (XXX and XXX) independently evaluated anonymized scans for pathological lesions, with discordant interpretations resolved through consensus discussion involving a third senior reader (XXX). Pathological neuroblastoma lesions were defined as focal areas of [^{18}F]FDG or [^{18}F]mFBG uptake in soft tissue or bone/bone marrow that exceeding both adjacent tissues

and contralateral reference areas, while absence of such distinct focal activity was classified as negative (24, 27, 28). To minimize confounding factors in [^{18}F]FDG interpretation, strict protocols were implemented (1): comprehensive prescan clinical assessments documenting surgical history, treatment timelines, and recent febrile/activity status; and (2) expert image analysis applying stringent diagnostic criteria that classified diffuse low-to-moderate bone marrow uptake as negative (especially during post-treatment recovery), with all findings clinically correlated. Quantitative analysis measured maximum/mean standardized uptake values ($SUV_{max/mean}$) for both lesions and normal organ backgrounds, enabling comparison of [^{18}F]mFBG and [^{18}F]FDG detection performance. Tumor-to-background ratios (TBR) were calculated by dividing lesion SUV_{max} by site-specific background SUV_{mean} (liver for hepatic lesions, bone/bone marrow for bone/bone marrow lesions, gluteal muscle for other lesions) (24, 29).

Statistical analysis

Owing to the low prevalence of neuroblastoma, the sample size recruited was determined by practical considerations. For continuous data, normality tests (Shapiro - Wilk test) were performed. Data meeting normal distribution criteria are now presented as mean ± standard deviation (SD), while non - normal data retain the median and range description. Differences in lesion detection per region and lesion uptake were analyzed using Mann - Whitney U test between [^{18}F]mFBG PET/CT and [^{18}F]FDG PET/CT studies. The McNemar test and Mann - Whitney U tests was employed to compare the diagnostic performance and TBR values of the two techniques, respectively. Statistical analyses were performed using SPSS software (version 26, SPSS Inc., Chicago, IL, USA). The statistical significance was defined as a p-value <0.05.

Results

Clinical characteristics of the participants

Sixty-five pediatric patients with neuroblastoma who underwent PET/CT imaging were initially enrolled. After applying exclusion criteria, 56 patients (28 females and 28 males, mean age 47.6 ± 38.0 months, range 6–108 months) were included in the final analysis. Exclusion criteria comprised: 6 patients who failed to complete both [^{18}F]mFBG and [^{18}F]FDG PET/CT scans, and 3 patients whose paired scans exceeded the one-week interval requirement. Notably, two children underwent a second set of paired scans during treatment response assessment, resulting in a total of 58 analyzable [^{18}F]FDG-[^{18}F]mFBG PET/CT scan pairs. The clinical indications for scanning included: treatment response evaluation (33 scans, 56.89%), pretreatment staging (14 scans, 24.14%), end-of-therapy assessment (6 scans, 10.34%), follow-up monitoring (4 scans, 6.89%), and recurrence detection (1 scan, 1.72%) (Figure 1, Table 1).

The primary tumor distribution analysis revealed 45 retroperitoneal cases, with remaining sites including mediastinum

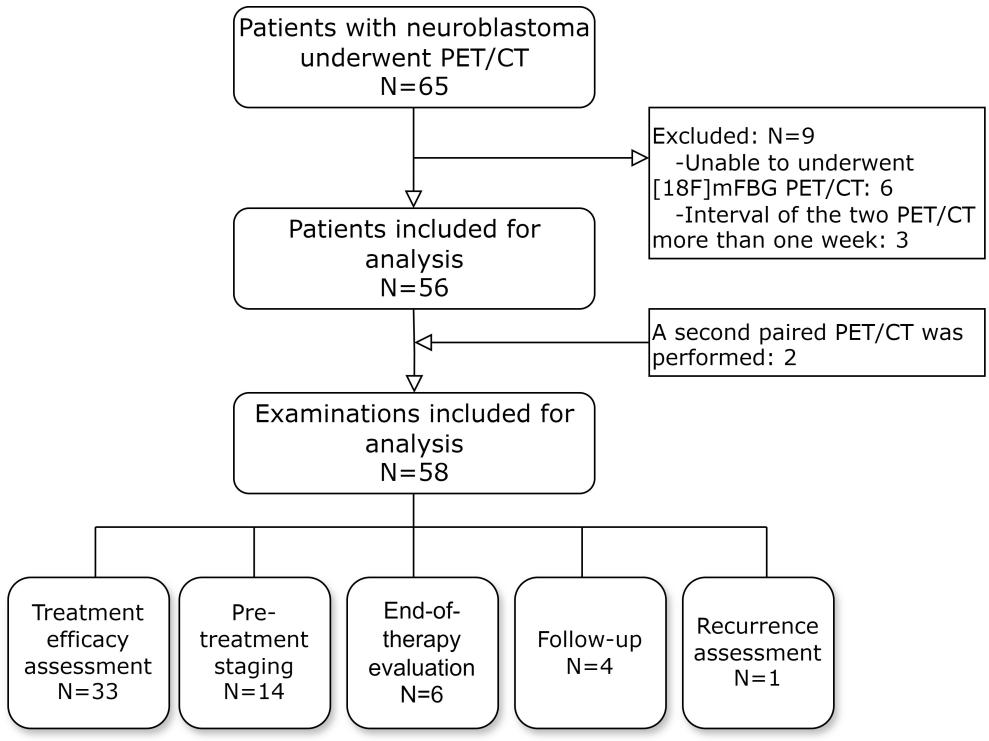

FIGURE 1
The flow diagram shows participant selection details.

TABLE 1 Patients and tumor characteristics.

Characteristics	[18F]mFBG PET/CT			[18F]FDG PET/CT		
	Positive (N=36)	Negative (N=20)	Total (N=56)	Positive (N=30)	Negative (N=26)	Total (N=56)
Age (months*)	50 ± 28.7 (9–106)	44.5 ± 27.3 (6–108)	47.6± 28.0 (6–108)	47.2 ± 28.9 (6–106)	46.1 ± 26.1 (12–108)	47.6± 28.0 (6–108)
Gender						
Male	20	8	28	18	10	28
Female	16	12	28	12	16	28
INRG Stage						
L1	10	1	11	9	2	11
L2	4	7	11	5	6	11
M	22	12	34	16	18	34
Risk						
Low	11	1	12	10	2	12
Intermediate	3	6	9	4	5	9
High	22	13	35	16	19	35
Indication for scan (58 paired scans)	Positive (N=37)	Negative (N=21)	Total (N=58)	Positive (N=30)	Negative (N=28)	Total (N=58)
Initial staging	14	0	14	14	0	14
Treatment efficacy assessment	20	13	33	14	19	33
EOT assessment	2	4	6	1	5	6
Follow-up	0	4	4	0	4	4
Recurrence	1	0	1	1	0	1

*Age is expressed as the mean± SD, with a range in parentheses. INRG, International Neuroblastoma Risk Group; EOT, end-of-therapy.

(n=4), pelvis (n=2), neck (n=2) and paravertebral/epidural area (n=2), and spermatic cord(n=1). Notably, the spermatic cord has not been previously reported as a primary site for neuroblastoma. According to the International Neuroblastoma Risk Group (INRG) staging system, 34 patients (60.71%) presented with stage M disease, while 35 patients (62.50%) were classified as high-risk. The median number of prior chemotherapy cycles at imaging was 6 (range 0-10).

No related adverse effects were observed following [18F]mFBG administration. Scan duration showed no significant difference between modalities ([18F]mFBG: 7.4 ± 2.8 min vs. [18F]FDG: 7.2 ± 3.0 min). Sedation was administered to 11 children during [18F]mFBG scans (mean age 1.8 ± 0.8 years) and 10 children during [18F]FDG scans (mean age 1.6 ± 1.0 years).

Comparison of detection sensitivity between [18F]mFBG PET/CT and [18F]FDG PET/CT: patient-based analysis

Twenty paired scans demonstrated concordant negative findings (13 treatment response evaluations, 4 EOT, and 3 follow-up scans), consistent with disease remission. Discordant results included 8 [18F]mFBG-positive/[18F]FDG-negative scans and 1 [18F]FDG-positive/[18F]mFBG-negative scan, while 29 scans showed positive on both modalities. The overall concordance rate between [18F]mFBG and [18F]FDG PET/CT was 84.48% (49/58) (representative examples shown in Figure 2).

Patient-based analysis revealed [18F]mFBG PET/CT detected significantly more soft tissue and skeletal lesions (63.79%, 37/58) compared to [18F]FDG PET/CT (51.72%, 30/58, p=0.039), with the difference being particularly pronounced in chemotherapy-treated patients. In the treatment response evaluation subgroup (n=33), [18F]mFBG demonstrated superior detection rates (60.60%, 20/33) versus [18F]FDG (42.42%, 14/33, p=0.031). However, no significant difference emerged between modalities (p=1.000) for initial staging (n=14), EOT evaluation (n=6), follow-up (n=4), or recurrence assessment (n=1) subgroups (combined detection rates: [18F]mFBG 68.00% [17/25] vs. [18F]FDG 64.00% [16/25]). Among 34 M-stage patients, [18F]mFBG maintained significantly higher positivity rates (64.70%, 22/34) than [18F]FDG (47.06%, 16/34, p=0.031).

Histopathological confirmation was obtained for six of eight [18F]mFBG-positive/[18F]FDG-negative cases, all verifying active

neuroblastoma (Figure 3). Conversely, the solitary [^{18}F]FDG-positive/[^{18}F]mFBG-negative cases showed no malignant cells on pathological examination (Figure 4).

Lesion-based comparative analysis of [^{18}F]mFBG and [^{18}F]FDG PET/CT performance

The lesion-based evaluation demonstrated superior detection capability of [^{18}F]mFBG PET/CT, which identified 431 total lesions (130 soft tissue, 301 skeletal) in 37 positive scans, compared to only 162 lesions (86 soft tissue, 76 skeletal) detected by [^{18}F]FDG PET/CT in 30 positive scans (Figure 5). Among 29 scan pairs positive on both modalities, [^{18}F]mFBG showed greater sensitivity for soft tissue lesions in 11 cases (37.93%), equivalent detection in 16 cases (55.17%), and reduced detection in 2 cases (6.89%), while for skeletal lesions it demonstrated superior detection in 23 cases (79.31%), comparable results in 4 cases (13.79%), and inferior performance in 2 cases (6.89%). Stratified analysis by INRG stage revealed comparable performance in early-stage (L1/L2) and low/intermediate-risk patients, while [^{18}F]mFBG significantly outperformed [^{18}F]FDG in metastatic (M stage) and high-risk groups (Table 2). Although both modalities detected more lesions at initial diagnosis and treatment response evaluation, only the efficacy assessment subgroup reached statistical significance.

Quantitative analysis showed significantly higher mean TBR for [^{18}F]mFBG (6.68 ± 5.76) versus [^{18}F]FDG (4.49 ± 2.88, p<0.001), with particularly notable differences in skeletal lesions ([^{18}F]mFBG 6.72 ± 6.06 vs. [^{18}F]FDG 3.26 ± 1.71, p<0.001) compared to soft tissue lesions ([^{18}F]mFBG 6.56 ± 4.88 vs. [^{18}F]FDG 5.71 ± 2.88, p=0.180).

Clinical impact on therapeutic decision-making

The detection discrepancy between imaging modalities significantly influenced treatment strategies in three of eight [^{18}F]mFBG-positive/[^{18}F]FDG-negative cases, promoting therapeutic modifications involving surgical intervention followed by systemic therapy. The remaining five cases, while confirming skeletal metastases through [^{18}F]mFBG imaging, maintained their original staging, risk classification, and treatment protocols.

A representative case involved a patient with primary right cervical neuroblastoma (initially staged as non-metastatic) whose post-operative [^{18}F]mFBG PET/CT revealed previously undetected

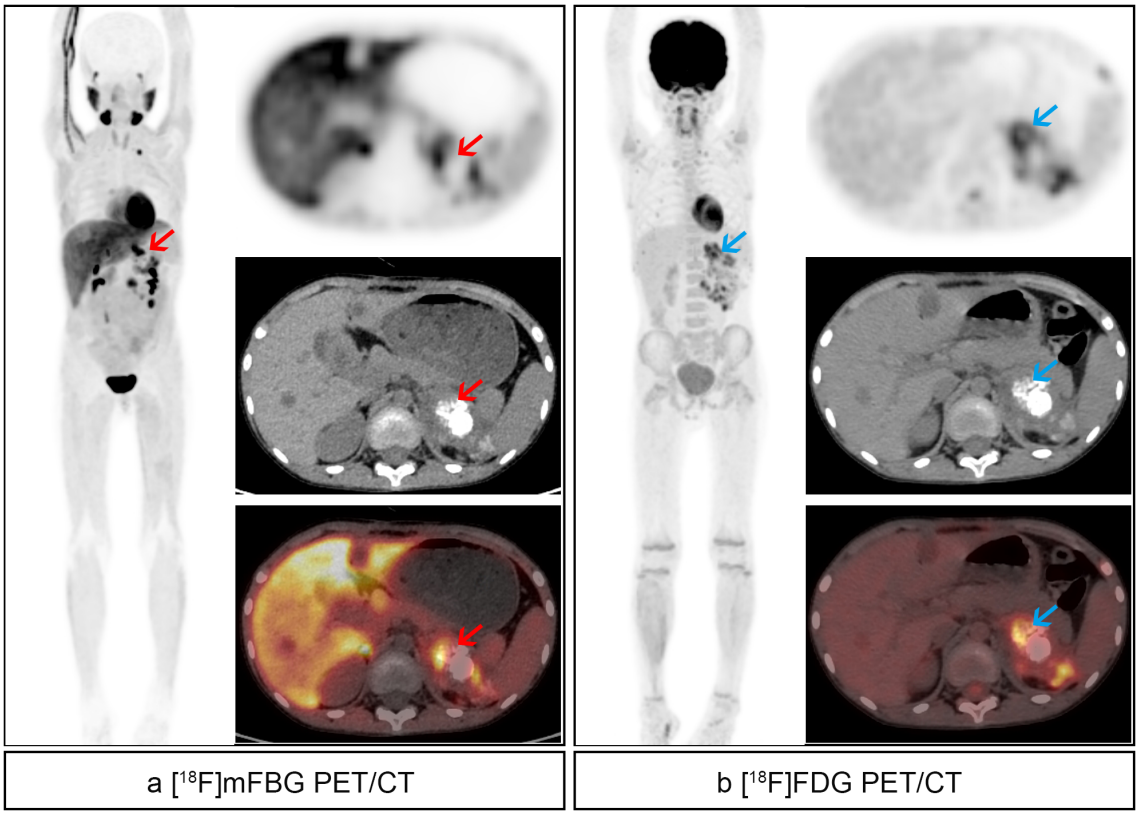

FIGURE 2
An 8-year-old boy with high-risk left retroperitoneal neuroblastoma received 1 cycle of chemotherapy. **(a)** [^{18}F]mFBG images. Pathological uptake (red arrows) with SUVmax 8.9 and TBR 12.5 was noted in the left retroperitoneal mass, and detailed showed in axial images. **(b)** [^{18}F]FDG images. Pathological uptake (blue arrows) with SUVmax 5.8 and TBR 11.9 was noted in the left retroperitoneal mass, and detailed show in axial images. Besides, residual activity of mFBG and FDG was found in the left thoracic entrance and retroperitoneal lymph nodes.

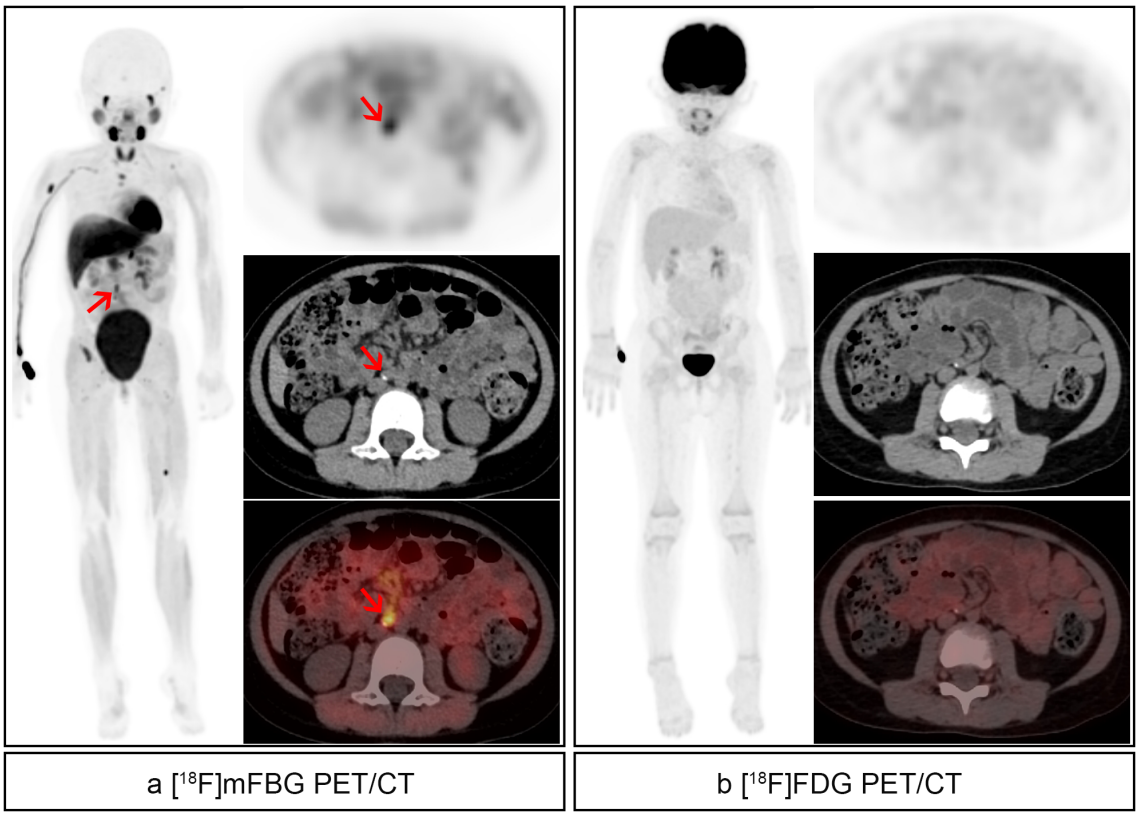

FIGURE 3
A 3-year-old girl suffered high-risk right retroperitoneal neuroblastoma with bone metastases and underwent resection of lesions followed by 8 cycles of chemotherapy. Post-therapy images were acquired. **(a)** [^{18}F]mFBG images. Pathological uptake (red arrows) with SUVmax 5.1 and TBR 4.9 was noted in the abdominal paraaortic lymph nodes, and detailed showed in axial images. And residual activity of mFBG was found in bone/bone marrow in multiple parts of the body. **(b)** [^{18}F]FDG images. No pathological uptake was found.

tibial metastases (upstaged to M), subsequently receiving chemotherapy, whereas concurrent [^{18}F]FDG imaging only demonstrated expected inflammatory uptake at the surgical site. Conversely, the solitary [^{18}F]FDG-positive/[^{18}F]mFBG-negative case underwent parent-requested surgical excision that histopathologically confirmed the absence of malignant cells, validating the [^{18}F]mFBG negative finding.

Discussion

This prospective study evaluated the diagnostic performance of [^{18}F]mFBG PET/CT in 56 neuroblastoma patients through 58 paired scans with [^{18}F]FDG PET/CT, demonstrating excellent safety with no adverse reactions observed. Both modalities showed comparable acquisition times (approximately 7 minutes), consistent with prior reports (24, 25). Our findings reveal [^{18}F]mFBG's superior diagnostic sensitivity versus [^{18}F]FDG in both patient-based (63.79% [37/58] vs. 51.72% [30/58], p=0.039) and lesion-based analyses (431 vs. 162 lesions detected, p<0.001). Quantitative assessment showed significantly higher mean TBR for [^{18}F]mFBG (6.68 ± 5.76) compared to [^{18}F]FDG (4.49 ± 2.88, p<0.001), with particularly notable differences in skeletal lesion detection. Pathological confirmation was obtained in seven surgically-treated cases (per parental request), with six [^{18}F]mFBG-positive/[^{18}F]FDG-negative lesions histologically verified as neuroblastoma, while the single [^{18}F]FDG-positive/[^{18}F]mFBG-negative case showed no malignant evidence. These results substantiated [^{18}F]mFBG PET/CT's superior specificity for post-treatment evaluation, suggesting its potential as a more reliable imaging biomarker than [^{18}F]FDG PET/CT for therapeutic monitoring in neuroblastoma patients.

Our results demonstrate that [^{18}F]mFBG PET/CT outperformed [^{18}F]FDG PET/CT in detecting skeletal lesions, identifying 269 additional metastases, including skull lesions that were obscured by physiological [^{18}F]FDG uptake (Figure 6). The statistically superior performance in treatment response assessment (compared to initial staging) likely reflects the predominance of early-stage disease (9 L1, 3 L2, and only 2 M stage cases) in our staging cohort, where lower lesion burden limited comparative sensitivity. Several methodological constraints must be acknowledged, including limited histopathological validation due to ethical and practical biopsy restrictions, lack of direct comparison with [^{123}I]MIBG imaging, and reliance on CT/MRI and clinical follow-up rather than pathological confirmation. These limitations highlight the necessity for future multi-center prospective trials to validate [^{18}F]mFBG PET/CT against [^{123}I]MIBG SPECT/CT, define its role in comprehensive

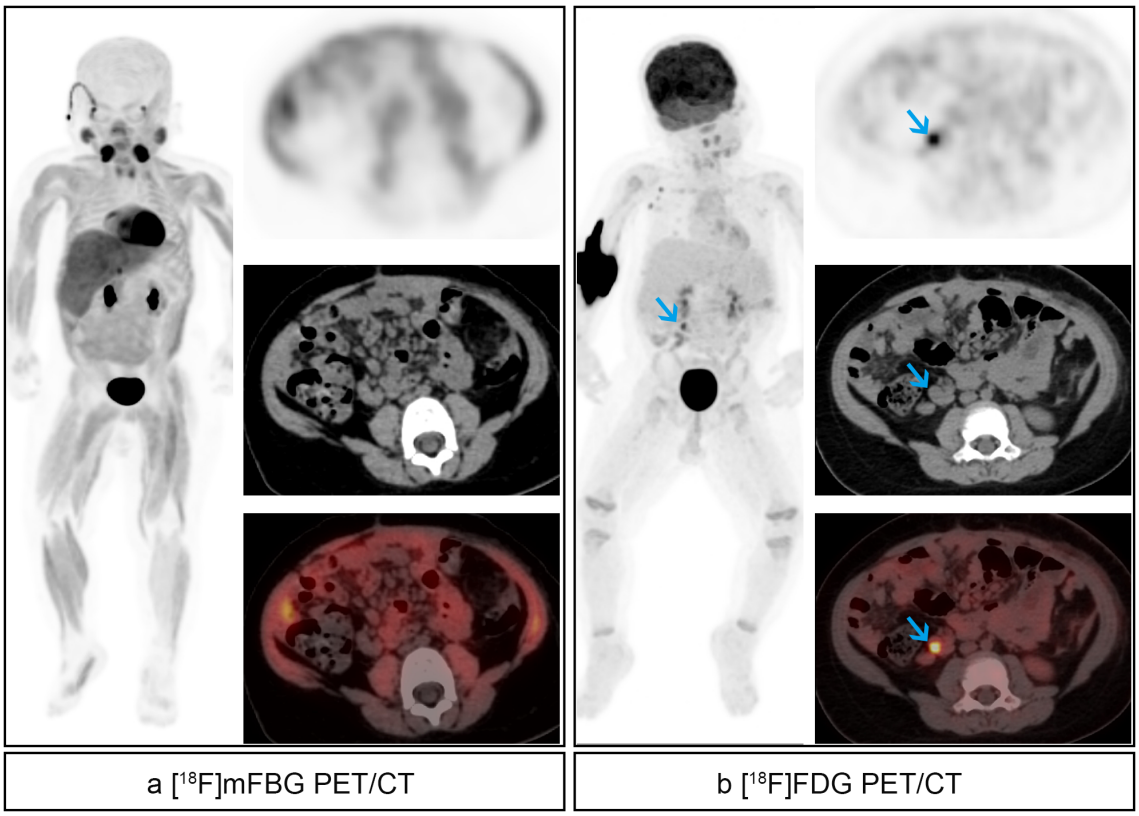

FIGURE 4
A 2-year-old boy suffered low-risk left retroperitoneal neuroblastoma and followed by 2 cycles of chemotherapy. Post-therapy images were acquired. **(a)** [^{18}F]mFBG images. No residual activity was found. **(b)** [^{18}F]FDG images. Abnormal activity (blue arrows) with SUVmax 5.0 and TBR 11.6 was found in the right retroperitoneal lymph node.

neuroblastoma assessment, and refine imaging protocols across different clinical scenarios.

Among the 35 patients categorized within the high-risk group, 28 exhibited poorly differentiated pathological types. The number of positive cases identified through [^{18}F]mFBG PET/CT and [^{18}F]FDG PET/CT was 17 and 13, respectively. Within the high-risk cohort, 10 cases demonstrated MYCN amplification, with 5 cases positive for [^{18}F]mFBG PET/CT and 4 for [^{18}F]FDG PET/CT. In the subgroup characterized by poorly differentiation and MYCN amplification, the difference in positivity rates between [^{18}F]FDG PET/CT and [^{18}F]mFBG PET/CT was not statistically significant, with P values of 0.125 and 1.00, respectively. Previous researches suggest that patients with poorly differentiated tumors and MYCN amplification were more likely to be MIBG-negative, indicating that they might particularly benefit from [^{18}F]FDG PET/CT imaging. However, this study did not observe a higher positivity rate for [^{18}F]FDG PET/CT, compared to [^{18}F]mFBG PET/CT in patients with poorly differentiated pathological types and MYCN amplification. This finding could be attributed to the limited sample size, alongside the fact that [^{18}F]mFBG PET/CT offers higher resolution and sensitivity than MIBG. Moreover, the criteria for high-risk classification encompass more than just differentiation status and MYCN amplification.

Two pediatric patients underwent sequential paired [^{18}F]FDG-[^{18}F]mFBG PET/CT scans at different therapeutic time points, with each scan pair analyzed independently. The follow-up [^{18}F]mFBG PET/CT demonstrated reduced tumor burden (both in lesion number and TBR values) compared to baseline scans, while [^{18}F]FDG PET/CT failed to show comparable treatment-related changes. This differential response pattern suggests [^{18}F]mFBG's superior utility for therapeutic monitoring. Furthermore, the technical advantages of [^{18}F]mFBG PET/CT - including superior spatial resolution and whole-body coverage - enabled enhanced tissue delineation and more precise anatomical localization of pathological uptake, even in regions adjacent to areas of physiological tracer accumulation (22, 25, 29, 30).

The administration of [^{18}F]mFBG in our study demonstrated an excellent safety profile, with all patients tolerating the procedure well - findings that align with previous clinical reports (25, 29, 31). Importantly, the majority of pediatric subjects (particularly valuable in neuroblastoma cases where most patients are <5 years old) successfully completed the imaging procedure without requiring sedation (32–34).

In our protocol, we selected a 1-hour post-injection acquisition time for PET/CT imaging to optimize patient convenience while maintaining diagnostic quality. This decision aligns with existing

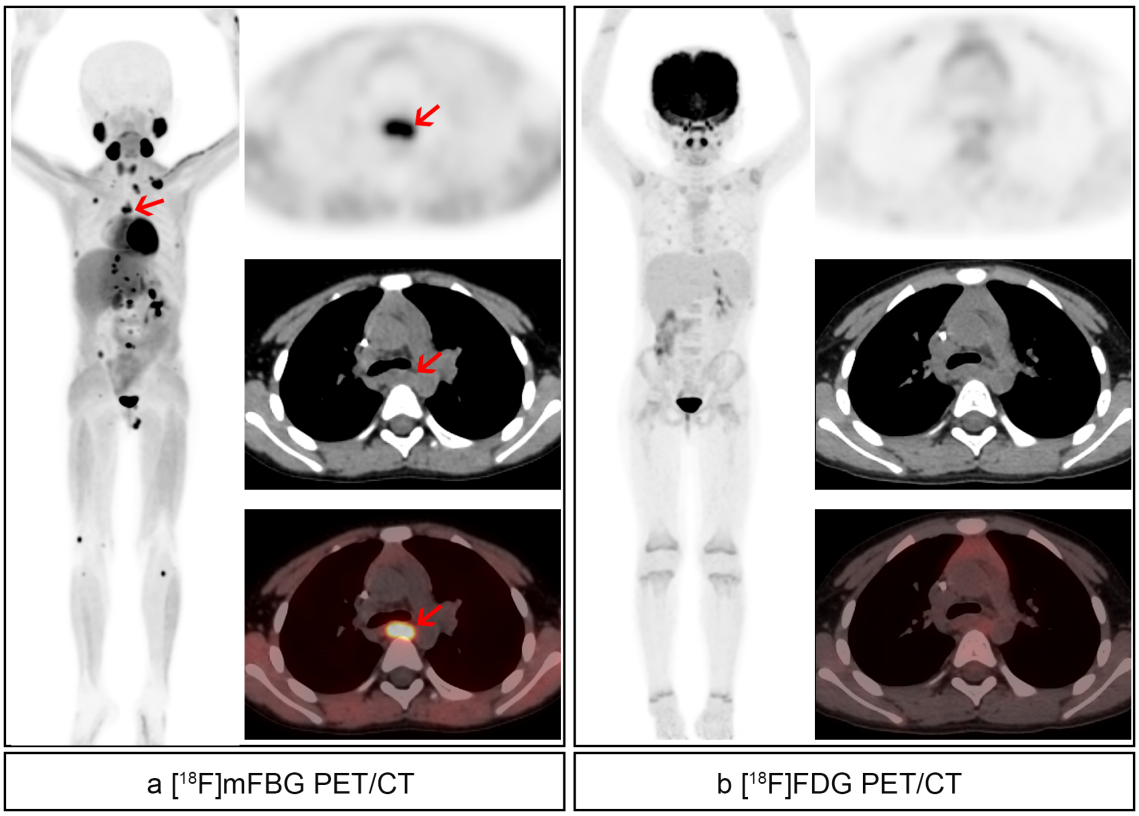

FIGURE 5
Therapy response evaluation of a 4-year-old boy suffered high-risk right retroperitoneal neuroblastoma underwent resection of lesions followed by 3 cycles of chemotherapy. **(a)** [^{18}F]mFBG images. Pathological uptake was found in extensive lymph nodes and bone/bone marrow (red arrows). **(b)** [^{18}F]FDG images. No residual activity was found.

TABLE 2 The number of lesions detected by two examination methods.

Characteristics	[^{18}F]FDG PET/CT			[^{18}F]mFBG PET/CT			P
	Soft tissues	BBM	Total	Soft tissues	BBM	Total	
INRG stage							
L1	14	0	14	14	0	14	P<1.00
L2	4	0	4	3	0	3	P<1.00
M	68	76	144	113	301	414	P<0.001
Risk group							
Low	15	0	15	15	0	15	P<1.00
Intermediate	3	0	3	2	0	2	P<1.00
High	68	76	144	113	301	414	P<0.001
Indication for scan							
Initial staging	28	9	37	30	34	64	0.18
Efficacy evaluation	51	67	118	94	265	359	0.001
EOT assessment	1	0	1	0	2	2	P<1.00
Follow-up	0	0	0	0	0	0	P<1.00
Recurrence	6	0	6	6	0	6	P<1.00

BBM, bone/bone marrow; INRG, International Neuroblastoma Risk Group; EOT, end of therapy.

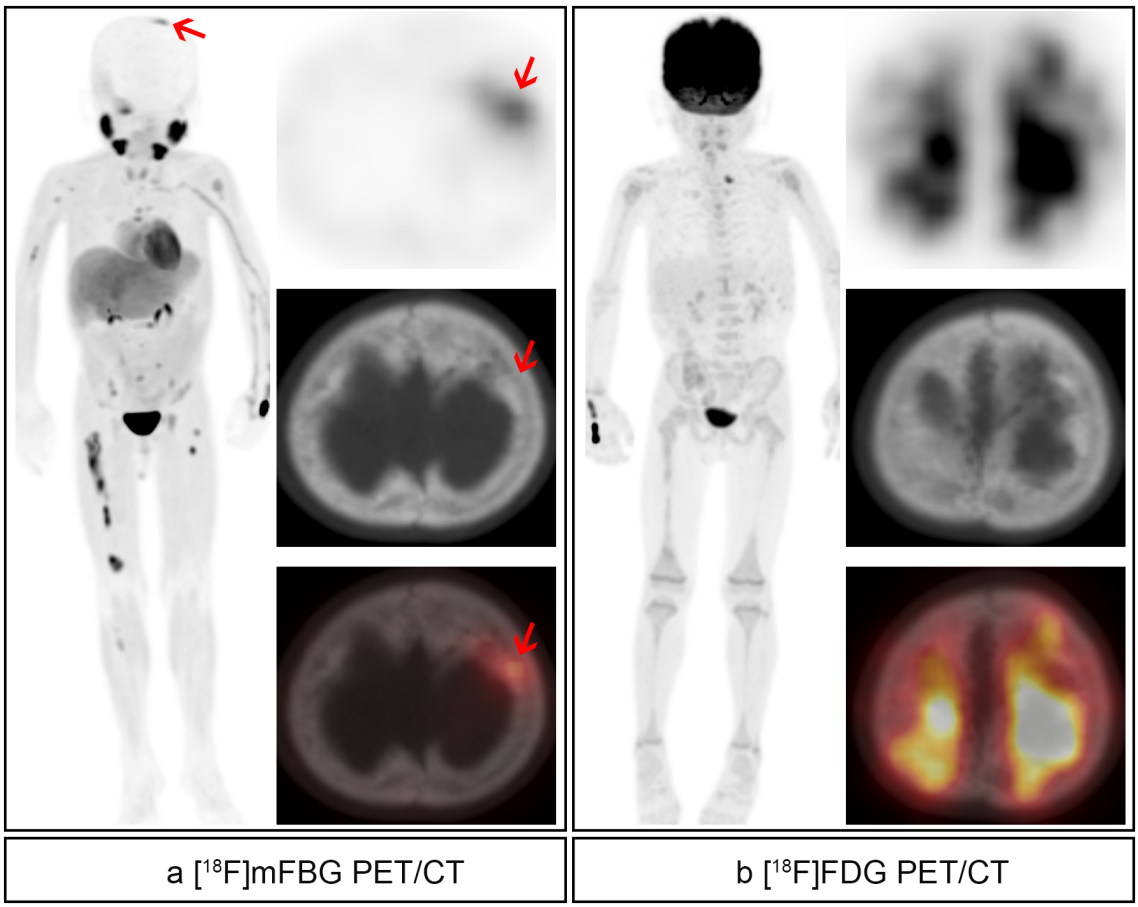

FIGURE 6
Therapy response evaluation of a 4-year-old boy with high-risk right retroperitoneal neuroblastoma underwent resection of lesions followed by 8 cycles of chemotherapy. **(a)** [^{18}F]mFBG images. Pathological uptake was found in the skull (red arrows). **(b)** [^{18}F]FDG images. No residual activity was found in the same site.

literature: Pandit-Taskar et al. demonstrated improved lesion detection and tumor-to-background contrast with scans obtained beyond 1-hour post-injection (22), while Atia Samim et al. Reported stable tumor uptake of [^{18}F]mFBG between 1–2 hours post-administration, with only minimal background uptake reduction at the later time-point (25).

Our study has several important limitations that should be acknowledged. The most significant constraint is the inability to directly compare our results with the current gold standard [^{123}I] MIBG SPECT/CT, primarily due to limited availability of this trace in many regions, especially Southwest China (6, 9, 35, 36). This highlights the urgent need for alternative PET tracers with enhanced diagnostic capabilities. Additionally, the relatively small sample size across different categories (End of Therapy, Follow-up, and Relapse) may introduce chance variations, limiting the reliability of statistical analyses. While [^{18}F]FDG PET/CT offers superior spatial resolution and is particularly valuable for MIBG-negative cases, its diagnostic value is compromised by nonspecific bone/bone marrow uptake during post-treatment recovery and intense physiological brain uptake, which can obscure true pathology (14, 15, 37–39). Another potential limitation of [18F] mFBG is its limited availability, as it requires cyclotron production, which may affect broader clinical implementation.

In our study, [^{18}F]mFBG PET/CT emerges as promising alternative, sharing the same norepinephrine transporter mechanism as [^{123}I]MIBG SPECT/CT while overcoming conventional limitations through PET's superior spatial resolution and quantitative capabilities (22, 24, 25, 32). However, the interpretation of our findings should consider that most patients (42/56) had undergone prior surgery and chemotherapy, which likely suppressed tumor metabolism and consequently reduced [^{18}F]FDG detection rates. To address these limitations, future studies should include more treatment-naïve patients and implement a synchronous trimodality imaging approach ([^{123}I] mIBG/[^{18}F]mFBG/[^{18}F]FDG) to minimize potential temporal biases and provide more comprehensive evaluations.

Conclusion

This pilot study highlights the superior diagnostic performance of [^{18}F]mFBG PET/CT over [^{18}F]FDG PET/CT in neuroblastoma

evaluation, suggesting that [^{18}F]FDG PET/CT should not be routinely used for this purpose. The significantly higher lesion detection rate with [^{18}F]mFBG PET/CT, particularly for skeletal metastases, has critical clinical implications for accurate staging and treatment monitoring. When [^{123}I]MIBG scintigraphy is unavailable, [^{18}F]mFBG PET/CT emerges as a more reliable alternative than [^{18}F]FDG PET/CT. Nevertheless, large-scale prospective trials directly comparing [^{18}F]mFBG PET/CT with the current gold-standard [^{123}I]MIBG imaging are warranted to validate these findings and potentially redefine standard neuroblastoma imaging protocols.

Data availability statement

The original contributions presented in the study are included in the article/supplementary material. Further inquiries can be directed to the corresponding authors.

Ethics statement

The studies involving humans were approved by institutional review boards of Children's Hospital of Chongqing Medical University. The studies were conducted in accordance with the local legislation and institutional requirements. Written informed consent for participation in this study was provided by the participants' legal guardians/next of kin.

Author contributions

WZ: Data curation, Writing – original draft. CY: Data curation, Methodology, Resources, Writing – original draft. ZZ: Data curation, Writing – original draft. SZ: Data curation, Writing – original draft. YH: Data curation, Writing – original draft. CZ: Data curation, Writing – original draft. YX: Data curation, Writing – original draft. CL: Data curation, Writing – original draft. YZ: Data curation, Writing – original draft. ZW: Data curation, Writing – original draft. LC: Supervision, Writing – review & editing. SW: Supervision, Writing – review & editing.

Funding

The author(s) declare financial support was received for the research and/or publication of this article. This work was supported by the Program for Youth Innovation in Future Medicine, Chongqing Medical University (no.W0155).

Conflict of interest

The authors declare that the research was conducted in the absence of any commercial or financial relationships that could be construed as a potential conflict of interest.

Generative AI statement

The author(s) declare that no Generative AI was used in the creation of this manuscript.

Any alternative text (alt text) provided alongside figures in this article has been generated by Frontiers with the support of artificial intelligence and reasonable efforts have been made to ensure accuracy, including review by the authors wherever possible. If you identify any issues, please contact us.

Publisher's note

References

1. Morgenstern DA, London WB, Stephens D, Volchenboum SL, Simon T, Nakagawara A, et al. Prognostic significance of pattern and burden of metastatic disease in patients with stage 4 neuroblastoma: A study from the International Neuroblastoma Risk Group database. *Eur J Cancer*. (2016) 65:1–10. doi: 10.1016/j.ejca.2016.06.005

2. Tas ML, Reedijk A, Karim-Kos HE, Kremer L, van de Ven CP, Dierselhuis MP, et al. Neuroblastoma between 1990 and 2014 in the Netherlands: Increased incidence and improved survival of high-risk neuroblastoma. *Eur J Cancer*. (2020) 124:47–55. doi: 10.1016/j.ejca.2019.09.025

3. Gatta G, Botta L, Rossi S, Aareleid T, Bielska-Lasota M, Clavel J, et al. Childhood cancer survival in Europe 1999-2007: results of EUROCARE-5–a population-based study. *Lancet Oncol*. (2014) 15:35–47. doi: 10.1016/S1470-2045(13)70548-5

4. Cohn SL, Pearson AD, London WB, Monclair T, Ambros PF, Brodeur GM, et al. The International Neuroblastoma Risk Group (INRG) classification system: an INRG Task Force report. *J Clin Oncol*. (2009) 27:289–97. doi: 10.1200/JCO.2008.16.6785

5. Pandit-Taskar N, Modak S. Norepinephrine transporter as a target for imaging and therapy. *J Nucl Med*. (2017) 58:39S–53S. doi: 10.2967/jnumed.116.186833

6. Park JR, Bagatell R, Cohn SL, Pearson AD, Villablanca JG, Berthold F, et al. Revisions to the international neuroblastoma response criteria: A consensus statement from the national cancer institute clinical trials planning meeting. *J Clin Oncol*. (2017) 35:2580–7. doi: 10.1200/JCO.2016.72.0177

7. Bagatell R, Park JR, Acharya S, Aldrink J, Allison J, Alva E, et al. Neuroblastoma, version 2.2024, NCCN clinical practice guidelines in oncology. *J Natl Compr Canc Netw*. (2024) 22:413–33. doi: 10.6004/jnccn.2024.0040

8. Bar-Sever Z, Biassoni L, Shulkin B, Kong G, Hofman MS, Lopci E, et al. Guidelines on nuclear medicine imaging in neuroblastoma. *Eur J Nucl Med Mol Imaging*. (2018) 45:2009–24. doi: 10.1007/s00259-018-4070-8

9. Liu B, Servaes S, Zhuang H. SPECT/CT MIBG imaging is crucial in the follow-up of the patients with high-risk neuroblastoma. *Clin Nucl Med*. (2018) 43:232–8. doi: 10.1097/RLU.0000000000001984

10. Wen Z, Zhang L, Zhuang H. Roles of PET/computed tomography in the evaluation of neuroblastoma. *PET Clin*. (2020) 15:321–31. doi: 10.1016/j.cpet.2020.03.003

11. Piccardo A, Morana G, Puntoni M, Campora S, Sorrentino S, Zucchetta P, et al. Diagnosis, treatment response, and prognosis: the role of (18)F-DOPA PET/CT in children affected by neuroblastoma in comparison with (123)I-mIBG scan: the first prospective study. *J Nucl Med*. (2020) 61:367–74. doi: 10.2967/jnumed.119.232553

12. Gains JE, Aldridge MD, Mattoli MV, Bomanji JB, Biassoni L, Shankar A, et al. 68Ga-DOTATATE and 123I-mIBG as imaging biomarkers of disease localisation in metastatic neuroblastoma: implications for molecular radiotherapy. *Nucl Med Commun*. (2020) 41:1169–77. doi: 10.1097/MNM.0000000000001265

13. Aboian MS, Huang SY, Hernandez-Pampaloni M, Hawkins RA, VanBrocklin HF, Huh Y, et al. (124)I-MIBG PET/CT to monitor metastatic disease in children with relapsed neuroblastoma. *J Nucl Med*. (2021) 62:43–7. doi: 10.2967/jnumed.120.243139

14. Bleeker G, Tytgat GA, Adam JA, Caron HN, Kremer LC, Hooft L, et al. 123I-MIBG scintigraphy and 18F-FDG-PET imaging for diagnosing neuroblastoma. *Cochrane Database Syst Rev*. (2015) 2015:CD009263. doi: 10.1002/14651858.CD009263.pub2

15. Sharp SE, Shulkin BL, Gelfand MJ, Salisbury S, Furman WL. 123I-MIBG scintigraphy and 18F-FDG PET in neuroblastoma. *J Nucl Med*. (2009) 50:1237–43. doi: 10.2967/jnumed.108.060467

16. Choi YJ, Hwang HS, Kim HJ, Jeong YH, Cho A, Lee JH, et al. (18)F-FDG PET as a single imaging modality in pediatric neuroblastoma: comparison with abdomen CT and bone scintigraphy. *Ann Nucl Med*. (2014) 28:304–13. doi: 10.1007/s12149-014-0813-1

17. Dhull VS, Sharma P, Patel C, Kundu P, Agarwala S, Bakhshi S, et al. Diagnostic value of 18F-FDG PET/CT in paediatric neuroblastoma: comparison with 131I-MIBG scintigraphy. *Nucl Med Commun*. (2015) 36:1007–13. doi: 10.1097/MNM.0000000000000347

18. Papathanasiou ND, Gaze MN, Sullivan K, Aldridge M, Waddington W, Almuhaideb A, et al. 18F-FDG PET/CT and 123I-metaiodobenzylguanidine imaging in high-risk neuroblastoma: diagnostic comparison and survival analysis. *J Nucl Med*. (2011) 52:519–25. doi: 10.2967/jnumed.110.083303

19. Zhao Z, Yang C. Predictive value of 18 F-FDG PET/CT versus bone marrow biopsy and aspiration in pediatric neuroblastoma. *Clin Exp Metastasis*. (2024) 41(5):627–38. doi: 10.1007/s10585-024-10286-2

20. Lu X, Li C, Wang S, Yin Y, Fu H, Wang H, et al. The prognostic role of (18)F-FDG PET/CT-based response evaluation in children with stage 4 neuroblastoma. *Eur Radiol*. (2024) 34(11):7125–35. doi: 10.1007/s00330-024-10781-w

21. Zhang H, Huang R, Cheung NK, Guo H, Zanzonico PB, Thaler HT, et al. Imaging the norepinephrine transporter in neuroblastoma: a comparison of [18F]-MFBG and 123I-MIBG. *Clin Cancer Res*. (2014) 20:2182–91. doi: 10.1158/1078-0432.CCR-13-1153

22. Pandit-Taskar N, Zanzonico P, Staton KD, Carrasquillo JA, Reidy-Lagunes D, Lyashchenko S, et al. Biodistribution and dosimetry of (18)F-meta-fluorobenzylguanidine: A first-in-human PET/CT imaging study of patients with neuroendocrine Malignancies. *J Nucl Med*. (2018) 59:147–53. doi: 10.2967/jnumed.117.193169

23. Piccardo A, Treglia G, Fiz F, Bar-Sever Z, Bottoni G, Biassoni L, et al. The evidence-based role of catecholaminergic PET tracers in Neuroblastoma. A systematic review and a head-to-head comparison with mIBG scintigraphy. *Eur J Nucl Med Mol Imaging*. (2024) 51:756–67. doi: 10.1007/s00259-023-06486-9

24. Wang P, Li T, Liu Z, Jin M, Su Y, Zhang J, et al. (18)F]MFBG PET/CT outperforming [(123)I]MIBG SPECT/CT in the evaluation of neuroblastoma. *Eur J Nucl Med Mol Imaging*. (2023) 50:3097–106. doi: 10.1007/s00259-023-06221-4

25. Samim A, Blom T, Poot AJ, Windhorst AD, Fiocco M, Tolboom N, et al. (18)F] mFBG PET-CT for detection and localisation of neuroblastoma: a prospective pilot study. *Eur J Nucl Med Mol Imaging*. (2023) 50:1146–57. doi: 10.1007/s00259-022-06063-6

26. Turnock S, Turton DR, Martins CD, Chesler L, Wilson TC, Gouverneur V, et al. (18)F-meta-fluorobenzylguanidine ((18)F-mFBG) to monitor changes in norepinephrine transporter expression in response to therapeutic intervention in neuroblastoma models. *Sci Rep*. (2020) 10:20918. doi: 10.1038/s41598-020-77788-3

27. Bai X, Wang X, Zhuang H. Increased gastric MIBG activity as a normal variant. *Clin Nucl Med*. (2019) 44:761–3. doi: 10.1097/RLU.0000000000002598

28. Bai X, Zhuang H. Focally increased MIBG activity in the muscle: real lesion or LOVENOX injection artifact. *Clin Nucl Med*. (2016) 41:167–8. doi: 10.1097/RLU.0000000000001000

29. Pauwels E, Celen S, Baete K, Koole M, Bechter O, Bex M, et al. (18)F] MFBG PET imaging: biodistribution, pharmacokinetics, and comparison with [(123)I] MIBG in neural crest tumour patients. *Eur J Nucl Med Mol Imaging*. (2023) 50:1134–45. doi: 10.1007/s00259-022-06046-7

30. Zhang W, Liu L, Yuan G, Deng M, Cai L. Comparison of 18 F-MFBG PET/CT and 18 F-FDG PET/CT images of metastatic neuroblastoma. *Clin Nucl Med*. (2024) 49:e480–480e481. doi: 10.1097/RLU.0000000000005226

31. Deng M, Shu Q, Hu M, Chen Y, Cai L. Comparison of 18 F-MFBG and 68 ga-DOTATATE PET/CT in the imaging of metastatic paraganglioma and pheochromocytoma. *Clin Nucl Med*. (2022) 47:e735–735e737. doi: 10.1097/RLU.0000000000004314

32. Borgwardt L, Brok J, Andersen KF, Madsen J, Gillings N, Fosbøl MØ, et al. Performing [18F]MFBG long-axial-field-of-view PET/CT without sedation or general anesthesia for imaging of children with neuroblastoma. *J Nucl Med*. (2024) 65:1286–92. doi: 10.2967/jnumed.123.267256

33. Botta L, Didonè F, Lopez-Cortes A, Nieto AC, Desandes E, Hjalgrim LL, et al. International benchmarking of stage at diagnosis for six childhood solid tumours (the BENCHISTA project): a population-based, retrospective cohort study. *Lancet Child Adolesc Health*. (2025) 9:89–99. doi: 10.1016/S2352-4642(24)00302-X

34. Nong J, Su C, Li C, Wang C, Li W, Li Y, et al. Global, regional, and national epidemiology of childhood neuroblastoma (1990-2021): a statistical analysis of incidence, mortality, and DALYs. *EClinicalMedicine*. (2025) 79:102964. doi: 10.1016/j.eclinm.2024.102964

35. Samim A, Tytgat G, Bleeker G, Wenker S, Chatalic K, Poot AJ, et al. Nuclear medicine imaging in neuroblastoma: current status and new developments. *J Pers Med*. (2021) 11. doi: 10.3390/jpm11040270

36. Vik TA, Pfluger T, Kadota R, Castel V, Tulchinsky M, Farto JC, et al. (123)I-mIBG scintigraphy in patients with known or suspected neuroblastoma: Results from a prospective multicenter trial. *Pediatr Blood Cancer*. (2009) 52:784–90. doi: 10.1002/pbc.21932

37. Melzer HI, Coppenrath E, Schmid I, Albert MH, von Schweinitz D, Tudball C, et al. ^{123}I-MIBG scintigraphy/SPECT versus ^{18}F-FDG PET in paediatric neuroblastoma. *Eur J Nucl Med Mol Imaging*. (2011) 38:1648–58. doi: 10.1007/s00259-011-1843-8

38. Tolboom N, Servaes SE, Zhuang H. Neuroblastoma presenting as non-MIBG-avid widespread soft tissue metastases without bone involvement revealed by FDG PET/CT imaging. *Clin Nucl Med*. (2017) 42:643–4. doi: 10.1097/RLU.0000000000001701

39. Wartski M, Jehanno N, Michon J, de Labriolle-Vaylet C, Montravers F. Weak uptake of 123I-MIBG and 18F-FDOPA contrasting with high 18F-FDG uptake in stage I neuroblastoma. *Clin Nucl Med*. (2015) 40:969–70. doi: 10.1097/RLU.0000000000000957